ACS OMEGA

http://pubs.acs.org/journal/acsodf

Article

Assessment of the Antileishmanial Potential of *Cassia fistula* Leaf Extract

Shams Tabrez, Fazlur Rahman, Rahat Ali, Abdulaziz S. Alouffi, Bader Mohammed Alshehri, Fahdah Ayed Alshammari, Mohammed A. Alaidarous, Saeed Banawas, Abdul Aziz Bin Dukhyil, and Abdur Rub*

Cite This: *ACS Omega* 2021, 6, 2318−2327

Read Online

ACCESS | Metrics & More | Article Recommendations | Supporting Information

ABSTRACT: *Cassia fistula* has a wide array of biologically active and therapeutically important class of compounds. *Leishmania donovani* important drug targets, sterol 24-c methyltransferase (*Ld*SMT), trypanothione reductase (*Ld*TR), pteridine reductase (*Ld*PTR1), and nucleoside hydrolase (*Ld*NH), were modelled, and molecular docking was performed against the abundant phytochemicals of its leaf extract. Molecular docking results provided the significant prima facie evidence of the leaf extract to have antileishmanial potential. To confirm this, we performed *in vitro* antileishmanial and cytotoxicity assays. Methanolic extract of *C. fistula* leaves showed growth inhibition and proliferation of *L. donovani* promastigote with an IC_{50} value of 43.31 ± 4.202 μg/mL. It also inhibited the growth of intra-macrophagic amastigotes with an IC_{50} value of 80.76 ± 3.626 μg/mL. *C. fistula* extract was found cytotoxic at a very high concentration on human macrophages (CC_{50} = 626 ± 39 μg/mL). Annexin V/propidium iodide (PI) staining assay suggested partial apoptosis induction in parasites by *C. fistula* to exert its antileishmanial activity. Here, for the first time, we have shown the antileishmanial potential of *C. fistula* leaves. Overall, our results could open new insight for an affordable and natural antileishmanial with high efficacy and less toxicity.

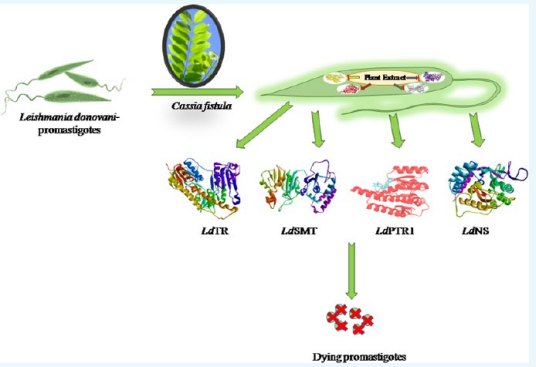

1. INTRODUCTION

Leishmaniasis is a vector-borne complex parasitic disease caused by obligate intramacrophagic protozoan parasite *Leishmania*. Leishmaniasis is a major global health problem threatening almost 350 million people worldwide with about 1.2−2 million new cases reported annually.[1] Leishmaniasis is manifested in three clinical forms: visceral, mucocutaneous, and cutaneous; the visceral form is the severest with approximately 500 000 new cases reported annually.[2] Visceral leishmaniasis (VL) or kala azar, is a lethal, chronic neglected tropical disease caused by intracellular protozoan parasites *Leishmania infantum* and *Leishmania donovani*. VL is endemic in more than 80 countries; however, about 80% of new VL cases worldwide are reported from the Indian subcontinent (India, Nepal, and Bangladesh).[3] If left untreated, VL becomes fatal. There is no vaccine available for human leishmaniasis. Currently, VL is treated using leishmanicidal drugs such as paromomycin, amphotericin B, liposomal amphotericin (AmBisome), and only available oral drug miltefosine (MIL).[4] Initially, these drugs had shown promising efficacy, but current studies have reported relapse rates between 6.8 and 10.8% after 6 months post-chemotherapeutics in immunocompetent patients in India.[5,6] The higher pathogenicity of *L. donovani* was connected with both SSG treatment failure and relapse after MIL treatment.[7] Drug resistance is another complication associated with the available chemotherapeutics. In addition, the available drugs have limitations like high cost, least availability, toxicity, and painful route of administration. Therefore, there is a need for new therapeutic options. Plants and their constituents had been in use for primary health care since ancient times. *Cassia fistula* Linn belongs to the family Caesalpiniaceae usually known as Amulthus and has been broadly used for the treatment and prevention of diseases in different types of traditional medicines. It is also known as the golden shower and Indian laburnum.[8] *C. fistula* is a very common plant known for its various medicinal properties and is native to South Asia and grown in other parts of the world. Animal model-based studies have shown that *C. fistula* and their constituents play a role in disease management via modulation of biological activities.[8] *C. fistula* has been reported to have antifertility,[9] antipyretic, analgesic, anti-inflammatory, hypoglycemic effects, and antimicrobial activity.[10−14]

In the current study, first, we searched the literature for the mention of the chemical constituents of *C. fistula* leaf extracts

Received: November 18, 2020
Accepted: December 28, 2020
Published: January 11, 2021

through mass spectrometry techniques. There are around 12 different major molecules in the leaf extract of *C. fistula*.[15] Most of these phytoconstituents are flavonoids, and many of them have medicinal values including antimicrobial activities.[10−15] *p*-Coumaric acid is a phenolic acid of the hydroxycinnamic acid family that shows *in vitro* antiviral activity against hepatitis C virus at the initial stage and antileishmanial activity.[16,17] Syringaresinol is a furofuran-type lignin and shows antileishmanial activity.[18] Myricetin belongs to the flavonoid class of polyphenolic compounds that possesses antioxidant and is known for its nutraceutical values.[19] Myricetin exhibits antibacterial activity against Gram-negative bacteria and antiviral activity, acting as a strong inhibitor of reverse transcription of human immunodeficiency virus (HIV) and Rauscher murine leukemia virus (RLV).[19] Proanthocyanidins, recognized as condensed tannins, are a class of flavonoids present as an active compound in medicinal plants and occur as polymers of different oligomeric forms.[20] Furthermore, proanthocyanidins are known for their antibacterial, antiviral, and antileishmanial activities.[20] It has been reported that flavonoids are a potential candidate for leishmanicidal drugs.[21] *L. donovani* contain many significant enzymes, which are considered as potential drug targets for the development of new therapeutic molecules. We have selected four key drug targets of *L. donovani* for molecular docking studies against the abundant phytochemicals of leaf extract. *Ld*PTR1 is an NADPH-dependent short-chain reductase responsible for the retrieval of pterins in the protozoan parasite *Leishmania*. This enzyme acts as a metabolic bypass for drugs targeting dihydrofolate reductase.[22] The *Ld*TR enzyme follows thiol-redox metabolism to keep trypanothione in its reduced form. This antioxidant property of *Ld*TR is essential for the survival of *L. donovani*.[23] *Ld*SMT is required for the biosynthesis of ergosterol, the major membrane sterol in *L. donovani*, responsible for parasite virulence, and highly conserved protein among *Leishmania* species.[24,25] *Ld*NH are conserved phylogenetic markers and important enzymes for the replication of DNA of the parasites.[26] We have selected these enzymes for molecular docking with major constituents of *C. fistula* for predicting the possible antileishmanial activity of these molecules. In silico approaches have been effectively used to predict protein structures and protein−ligand interactions. Molecular docking is a computational method used to speculate the preferred orientation of ligands (organic molecules) with the proteins. Accordingly, nature provides a huge diversity and an alternative source of valuable chemical structures for biological screening test against pathogens. We further tested our hypothesis through different antileishmanial and cytotoxicity assays on promastigotes, amastigotes, and human THP-1-derived macrophages.

2. MATERIAL AND METHODS

2.1. Molecular Docking Studies. PyRx was used for the virtual screening of the phytochemical compounds and target proteins of *L. donovani*.[27] The target protein was changed into a macromolecule, which converted the atomic coordinates into pdbqt format. The grid box was selected around the crystal structure while other parameters were left as default for molecular docking by AutoDock Vina.[28] The binding affinity and inhibitory constant were used to analyze the results of molecular docking, and then all possible docked conformations were generated for different constituents. The detailed interactions, including their types such as hydrogen bonding, van der Waals, alkyl, pi-alkyl, and halogen interactions, between different constituents and the target proteins were analyzed by BIOVIA Discovery Studio.[29] The most favorable binding poses of the compounds were analyzed by choosing the lowest free energy of binding (ΔG) and the lowest inhibition constant (Ki), which is calculated using the following formula:

$$Ki_{pred} = \text{exponential}^{(\Delta G/RT)}$$

where ΔG is the binding affinity (kcal/mol), R (gas constant) is 1.98 cal K^{-1} mol^{-1}, and T (room temperature) is 298.15 Kelvin.

2.2. Sequence Analysis, Template Identification, Homology Modeling, Receptor and Ligand Preparation. Due to the lack of solved three-dimensional (3D) structures of *Ld*TR, *Ld*NH, and *Ld*SMT, homology modeling was opted to determine the structure of these enzymes. The protein sequence of *Ld*TR, *Ld*NH, and *Ld*SMT enzymes of *L. donovani* was retrieved from NCBI. For the identification of similar templates, BlastP[30] was performed against Protein Data Bank (PDB), and on the basis of maximum sequence similarity and least *e*-value, the crystal structures were used as template structures to model the 3D structures. Modeller 9.24[31] was used for homology modeling, and 3D structures were visualized in PyMol. The generated models were assessed by the PROCHECK program, PDB sum tool, and Ramachandran plots.[32,33] The crystal structure of pteridine reductase protein was downloaded from PDB (ID: 2XOX). The proteins were finally prepared by Discovery Studio keeping all of the parameters at default. The critical residues of the binding pockets were identified from the native catalytic pockets of the available crystal structure of proteins, CASTp, and Discovery Studio. The 3D structure of the constituents of the leaf extract of *C. fistula* was retrieved from the PubChem database in SDF format.[34] Syringaresinol, quercetin-*O*-hexoside, and apigenin-*C*-hexoside-*O*-pentoside were sketched by MarvinSketch. The atomic coordinates of all of the ligands were changed to pdbqt setup using Open Babel GUI, an open-source chemical toolbox for the interconversion of chemical structures.[35] Universal Force Field (uff) was used for energy minimization.[36]

2.3. Chemicals and Reagents. M199 media for promastigote culturing, Roswell Park Memorial Institute (RPMI) 1640 media for the cell line, penicillin−streptomycin antibiotic cocktail, and fetal bovine serum (FBS) were procured from Gibco and Thermo Fisher Scientific, Inc., Waltham, MA. *N*-2-hydroxyethylpiperazine-*N*′-2-ethanesulfonic acid (HEPES), sodium bicarbonate, paraformaldehyde were obtained from Sigma-Aldrich, Saint Louis, MO. Miltefosine, 3-[4,5-dimethylthiazol-2-yl]-2,5 diphenyl tetrazolium bromide (MTT) assay reagents, and cell culture-grade dimethyl sulfoxide (DMSO) and other solvents for plant extract were from Merck & Co., Inc., Kenilworth, NJ. Propidium iodide and Annexin fluorescein isothiocyante (FITC) was procured from Thermo Fisher Scientific, Inc., Waltham, MA. All of the other chemicals and reagents were purchased from Sigma-Aldrich, Saint Louis, MO, or Merck & Co., Inc., Kenilworth, NJ, unless stated otherwise.

2.4. Promastigote Phase Parasites and THP-1 Cell Line Culture and Maintenance. *L. donovani* infective strain (MHOM/IN/83/AG83) was maintained in M199 media at pH 7.4 supplemented with 25 mM HEPES, 10% heat-inactivated FBS, and 1% penicillin−streptomycin antibiotic cocktail at a temperature of 22 °C. The log-phase parasite culture was passaged at regular intervals of 72−96 h with an inoculum density of 2×10^6 parasites per mL. THP-1 human

https://dx.doi.org/10.1021/acsomega.0c05629
ACS Omega 2021, 6, 2318−2327

Table 1. Molecular Docking Interaction of Abundant Medicinal Phytochemicals in the Liquid Chromatography−Mass Spectrometry (LC−MS) Analysis Data of *C. fistula* with the *L. donovani* Drug Target Proteins[a]

s. no.	proteins	ligands	binding energy (kcal/mol)	pKi_{pred} (μM)	no. of H-bonds	interacting residues
1.	sterol 24-*C*-methyltransferase	proanthocyanidin B dimer	−9.4	6.92	5	Asp168, Thr170, Phe264, Glu265, Ile272
		kaempferol rhamnosylxyloside	−9.3	6.84	8	Met237(2), Glu238(2), Leu297, Thr298(2), Arg309
		myricetin hexoside	−9.0	6.62	5	Asn163, Met164, Cys189, Val193, Ile258
		apigenin-6,8-di-*C*-glycoside	−8.9	6.55	4	Asp160, Asn163, Met164, Val193
2.	trypanothione reductase	proanthocyanidin B dimer	−8.4	6.18	4	Met70, Leu88(2), Ser87
		kaempferol rhamnosylxyloside	−8.2	6.03	4	Gly229, Met333, Val362, Gly376
		myricetin hexoside	−7.7	5.66	5	His359, Gly376, Thr378, Glu381(2)
		apigenin-*C*-hexoside-*O*-pentoside	−7.7	5.66	3	Thr374, Gly376(2)
3.	nucleoside hydrolase	proanthocyanidin B dimer	−7.8	5.74	2	Asn160, Thr238
		apigenin-*C*-hexoside-*O*-pentoside	−7.7	5.66	7	Thr158, Gly159, Asp192, His195(2), Gln196, Arg233
		3,4-di-*O*-caffeoylquinic acid	−7.6	5.59	5	His157, Thr158, Asp192, Arg233(2)
		kaempferol rhamnosylxyloside	−7.5	5.52	3	Asp192, His195, Arg233
4.	pteridine reductase	proanthocyanidin B dimer	−6.8	5.00	1	Glu256
		3,4-di-*O*-caffeoylquinic acid	−6.8	5.00	6	Val180, Tyr194, Lys198(2), Pro224, Asp280
		kaempferol rhamnosylxyloside	−6.5	4.78	2	Val279, Asp280
		apigenin-*C*-hexoside-*O*-pentoside	−6.1	4.49	2	Val180, Glu256

[a]Abbreviations: p*Ki*, negative decimal logarithm of inhibition constant; pred, predicted.

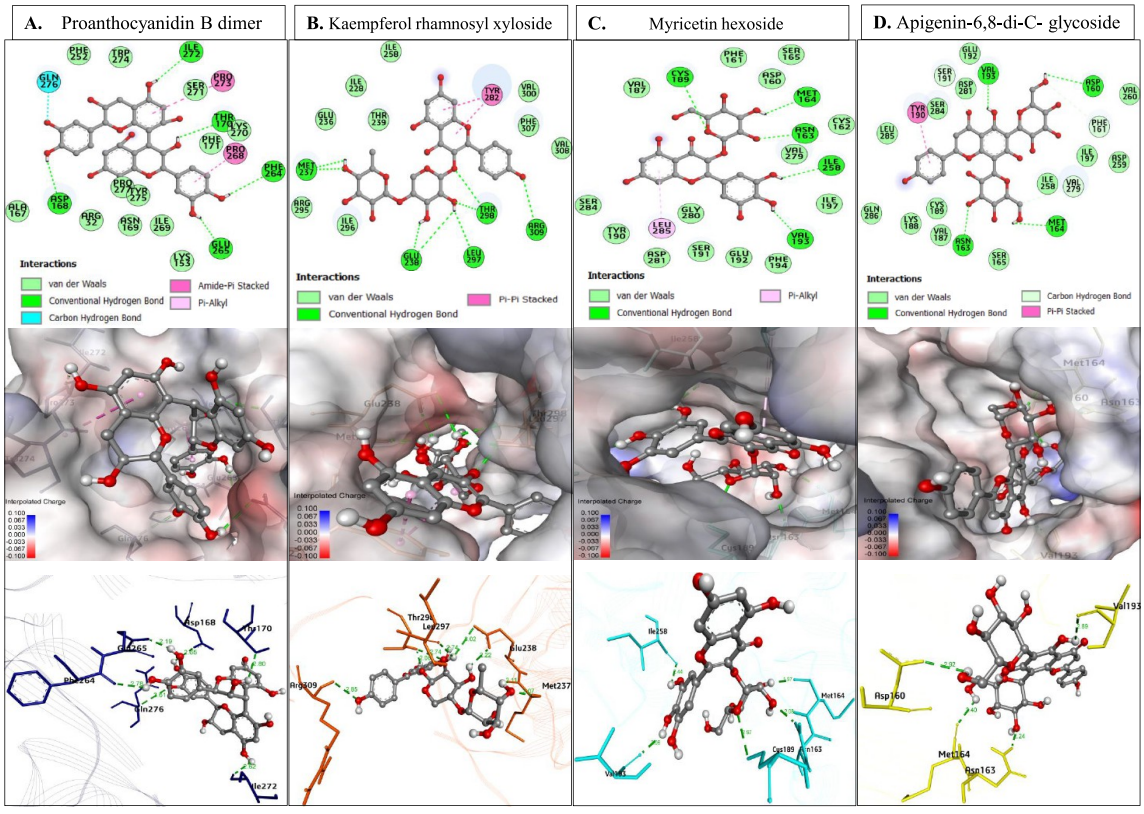

Figure 1. Binding pattern of *C. fistula* major chemical constituents with the SMT of *L. donovani*. Two-dimensional (2D) plot, surface representation of protein binding pocket residues, and its significant interactions with (A) proanthocyanidin B dimer, (B) kaempferol rhamnosylxyloside, (C) myricetin hexoside, and (D) apigenin-6,8-di-*C*-glycoside.

monocytic cell line was maintained in RPMI-1640 media supplemented with 10% FBS and 1% penicillin−streptomycin antibiotic in a humidified atmosphere in a CO_2 incubator at 5% CO_2 and 37 °C temperature. THP-1 monocytic cells were stimulated with 20 ng/mL of phorbol myristate acetate (PMA) for differentiation to macrophages.

2.5. Plant Extract Preparation. *C. fistula* leaves were collected from natural habitats, and the identification was done by Dr. Sunita Garg, Chief Scientist and Head, Herbarium Department, National Institute of Science Communication and Information Resources (NISCAIR), New Delhi, India (ref No. NISCAIR/RHMD/Consult/2018/3268-69-5). After collecting it from the field, selected plant materials were washed and air-dried in shade at room temperature. After the leaves were moisture-free, they were grounded separately in an electric grinder. The prepared powder form of plant materials (100 g)

https://dx.doi.org/10.1021/acsomega.0c05629
ACS Omega 2021, 6, 2318−2327

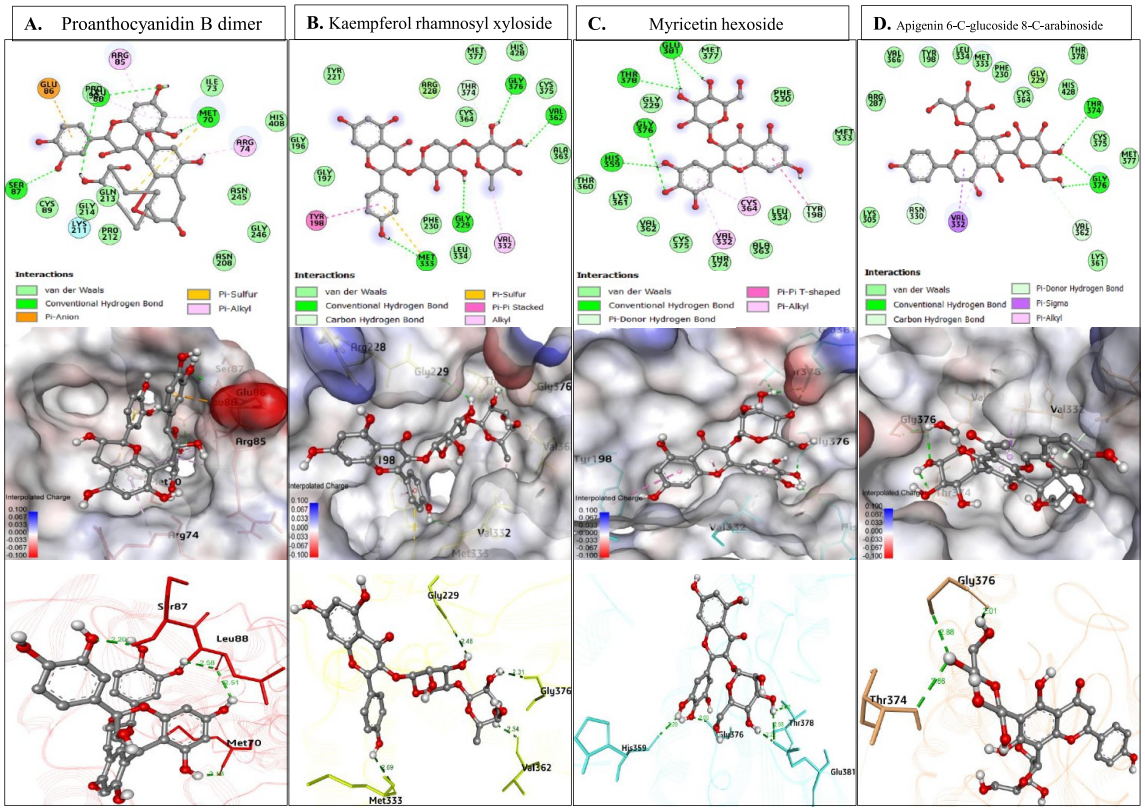

Figure 2. Binding pattern of *C. fistula* major chemical constituents with the TR of *L. donovani*. 2D plot, surface representation of protein binding pocket residues, and its significant interactions with (A) proanthocyanidin B dimer, (B) kaempferol rhamnosylxyloside, (C) myricetin hexoside, and (D) apigenin-6-*C*-glucoside 8-*C*-arabinoside.

was soaked in 500 mL of methanol and placed on a rotary shaker at room temperature for 24 h. The extract was filtered using a Buchner funnel and Whatman filter paper and concentrated to dryness using a rotary evaporator under vacuum at 35 °C. The dried plant extract was stored at −20 °C until used for bioassay.

2.6. IC_{50} Determination of *C. fistula* Leaf Extract. To check the antipromastigote activity of *C. fistula*, log-phase promastigotes were incubated at a density of 5×10^6 parasites in the presence and absence of leaf methanolic extract. To determine the IC_{50} value, parasites were incubated at different concentrations of extract. The percentage inhibition was calculated as (mean parasite number of treated sample/mean parasite of control) × 100. The IC_{50} value was determined by extrapolating the graph of % of viable parasites under treatment versus the concentration of extract.

2.7. Antiamastigote Assay and Cytotoxicity Evaluation of *C. fistula* Extract. Treatment of 2×10^6 differentiated macrophages with twofold serial dilution of extract was conducted for 24 h. Cells were incubated with 50 μM MTT for 3−4 h; thereafter, the resulting formazan was dissolved in 150 μM DMSO. The amount of formazan produced represented the relative number of viable cells and was recorded spectrophotometrically at 570 nm by an ELISA plate reader. The CC_{50} value (50% cell cytotoxic concentration) was defined by the graphical extrapolation of the dose−response curve of % viability against the plant extraction concentration. For parasite load study, 2×10^5 THP-1 cells were seeded on the coverslip, and after proper differentiation to macrophages using PMA, the adherent cells were infected with log-phase virulent promastigotes in a ratio of 1:10 (macrophage to *Leishmania*) for 24 h. The noninternalized parasites were washed, and the infected macrophages were further incubated with different concentrations of plant extract, for the next 24 h. The coverslips were washed, fixed with chilled methanol, and stained using a modified Giemsa stain for microscopic observation of amastigotes. About 100 macrophages were counted from different focus to determine the parasite burden.

2.8. Apoptotic Assay. *L. donovani* promastigotes (2×10^6) were incubated at different doses of plant extract (31.7, 62.5, and 125 μg/mL) and incubated for 48 h. Miltefosine at a dose of 3 μg/mL served as positive control, and parasites without treatment were considered as a negative control. Treated and untreated promastigotes were further centrifuged at 3000*g* for 5 min and washed three times in 1× PBS buffer. Further, the pellet was resuspended in 195 μL of 1× binding buffer (10 mM Hepes (pH 7.4), 140 mM NaCl, and 2.5 mM $CaCl_2$) containing 5 μL of annexin-FITC and 5 μL of propidium iodide for 25 min in the dark at room temperature in a dark room. After 25 min of incubation, the samples were analyzed through a BD FACSAria III Cell Sorter at excitation wavelengths of 488 and 550 nm.

2.9. Statistical Analysis. All of the experiments were performed in technical triplicate, and the results represented are the mean of the triplicate with scanning electron microscopy (SEM). Statistical analysis was performed using GraphPad Prism 7.0 software, and the statistical significance was calculated using one-way analysis of variance (ANOVA) followed by Dunnett's multiple comparison test. $P < 0.5$ was considered statistically significant.

3. RESULTS

3.1. Homology Modeling and Molecular Docking. The *Ld*SMT, *Ld*TR, and *Ld*NH drug targets were modeled using

https://dx.doi.org/10.1021/acsomega.0c05629
ACS Omega 2021, 6, 2318−2327

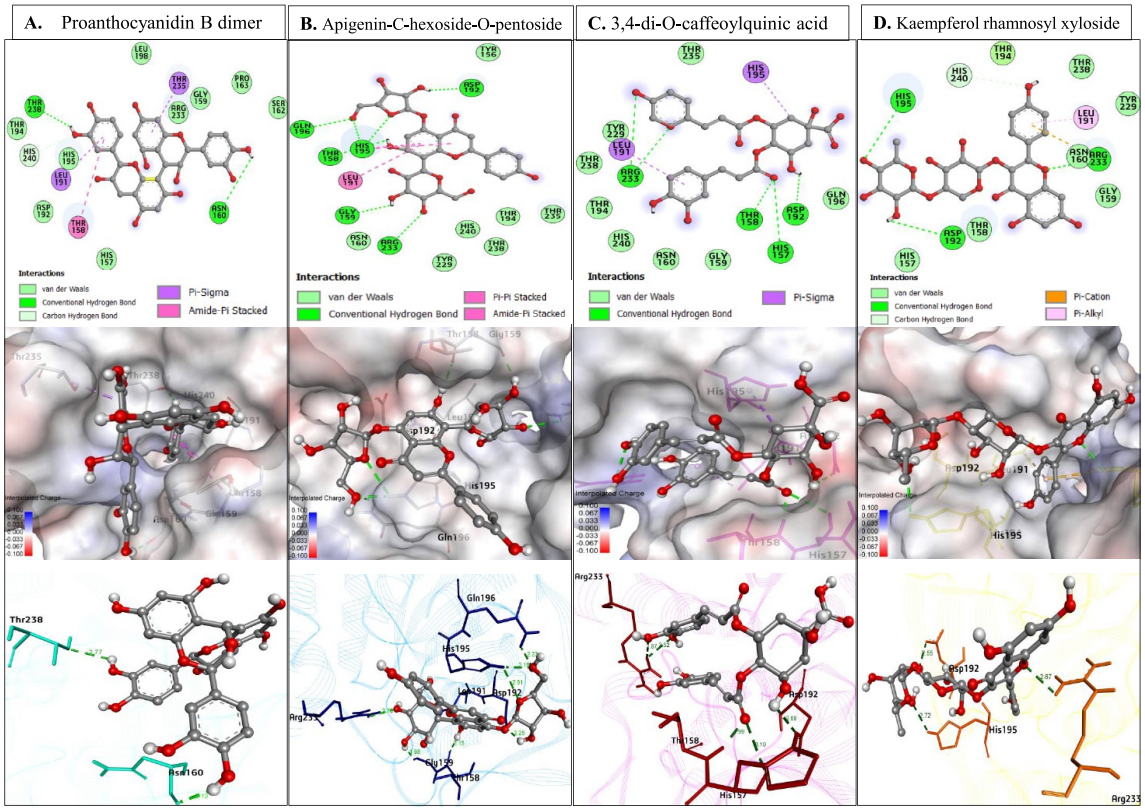

Figure 3. Binding pattern of *C. fistula* major chemical constituents with the NH of *L. donovani*. 2D plot, surface representation of protein binding pocket residues, and its significant interactions with (A) proanthocyanidin B dimer, (B) apigenin-*C*-hexoside-*O*-pentoside, (C) 3,4-di-*O*-caffeoylquinic acid, and (D) kaempferol rhamnosylxyloside.

Modeller 9.24 (Table S1). The best model among the hundred generated models was chosen based on the lowest score for the docking study. The energy minimization was carried out by the BIOVIA Discovery Studio. The three-dimensional cartoon representations of *Ld*SMT, *Ld*TR, and *Ld*NH are shown in Figures S1A−S3A, respectively. The generated models of *Ld*SMT, *Ld*TR, and *Ld*NH show stereochemical quality having 99.8, 100.0, and 99.0% residues in allowed regions and only 0.2, 0.0, and 1.0% residues in disallowed region of Ramachandran plot, respectively (Figures S1B−D, S2B−D, and S3B−D). CASTp and Discovery Studio were used to find the key residues and region around the binding cavity of *Ld*SMT, *Ld*TR, and *Ld*NH. The active-site residues of the *Ld*SMT, *Ld*TR, *Ld*NH, and *Ld*PTR1 enzymes making different numbers of hydrogen bonds within 3.5 Å as well as hydrophobic bonds within 5 Å of the ligands were identified. Among all kinds of various interactions like amide−π interactions, $\pi-\pi$, H-bond, etc., the binding efficiency is being evaluated on the idea of hydrogen bonding.[37,38] Virtual screening was performed against active-site residues of *Ld*SMT, *Ld*TR, *Ld*NH, and *Ld*PTR1 targets using PyRx. After the successful screening of the phytochemicals present in the methanolic leaf extract of *C. fistula*, the top ligands with the lowest binding energy were selected. Based on binding energy and inhibitory constant, six complexes having the highest binding affinities were carefully chosen for further analysis (Table 1). Proanthocyanidin B dimer has been found to possess the lowest binding energy and the highest binding affinity ranging from −9.4 to −6.8 kcal/mol against *Ld*SMT, *Ld*TR, *Ld*NH, and *Ld*PTR1 enzymes, as shown in Table 1. The binding pattern of the proanthocyanidin B dimer with *Ld*SMT, *Ld*TR, *Ld*NH, and *Ld*PTR1 may hinder the substrate accessibility and its subsequent inhibition, as shown in Figures 1−4 A. Proanthocyanidin B dimer interacts with the Asp168, Thr170, Phe264, Glu265, and Ile272 binding-site residues of *Ld*SMT by five intermolecular hydrogen bonds with bond lengths of 2.65, 2.80, 2.78, 2.19, 2.62, and 3.61 Å, respectively (Figure 1A). Proanthocyanidin B dimer interacts with the *Ld*TR, *Ld*NH, and *Ld*PTR1 enzymes by four, two, and one hydrogen bonds having bond lengths of 2.18, 2.20, 2.51, and 2.58; 2.13 and 2.77; and 2.39 Å, respectively, as represented in Figures 2−4A. Kaempferol rhamnosylxyloside has shown the second-highest binding energy between −9.3 and −6.5 kcal/mol against the targeted enzymes (Table 1). Kaempferol rhamnosylxyloside interacts with the Met237(2), Glu238(2), Leu297, Thr298(2), and Arg309 residues of *Ld*SMT by eight intermolecular hydrogen bonds having bond lengths of 2.07, 2.11, 2.22, 3.02, 2.74, 2.08, 2.74, and 2.85 Å, respectively (Figure 1B). Kaempferol rhamnosylxyloside interacts with *Ld*TR, *Ld*NH, and *Ld*PTR1 through four, three, and two hydrogen bonds having bond lengths of 2.48, 2.69, 2.34, and 2.31; 2.55, 2.72, and 2.67; and 2.70 and 2.77 Å, respectively, as shown in Figures 2B, 3D, and 4C. The Asn163, Met164, Cys189, Val193, and Ile258 residues of *Ld*SMT interact with Myricetin hexoside by five intermolecular hydrogen bonds having bond lengths of 2.08, 1.97, 2.97, 2.06, and 2.44 Å, respectively (Figure 1C). Apigenin-6,8-di-*C*-glycoside interacts with *Ld*SMT through four hydrogen bonds with bond lengths of 2.92, 2.24, 2.40, and 2.89 Å, as shown in Figure 1D. Myricetin hexoside interacts with *Ld*TR through five hydrogen bonds with bond lengths of 2.29, 2.60, 2.92, 2.22, and 2.95 Å, as shown in Figure 2C. Apigenin-6,8-di-*C*-glycoside interacts with the Asp160, Asn163, Met164, and Val193 residues of *Ld*SMT by eight intermolecular hydrogen

https://dx.doi.org/10.1021/acsomega.0c05629
ACS Omega 2021, 6, 2318−2327

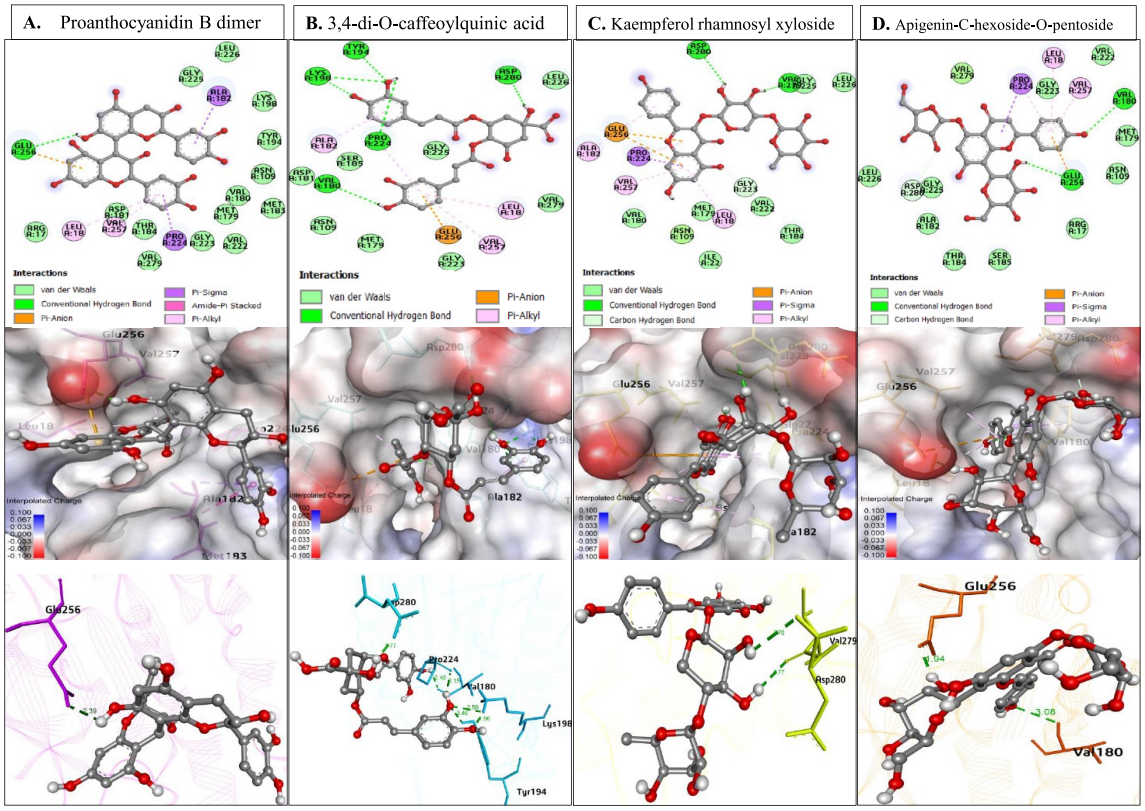

Figure 4. Binding pattern of *C. fistula* major chemical constituents with the PTR1 of *L. donovani*. 2D plot, surface representation of protein binding pocket residues, and its significant interactions with (A) proanthocyanidin B dimer, (B) 3,4-di-*O*-caffeoylquinic acid, (C) kaempferol rhamnosylxyloside, and (D) apigenin-*C*-hexoside-*O*-pentoside.

bonds having bond lengths of 2.92, 2.24, 2.40, and 2.89 Å, respectively (Figure 1D). Apigenin-C-hexoside-O-pentoside interacts with *Ld*TR, *Ld*NH, and *Ld*PTR1 by three, seven, and two intermolecular hydrogen bonds having bond lengths of 2.86, 2.01, and 2.88; 2.15, 1.98, 2.25, 2.19, 2.91, 2.23, and 2.70; and 3.08 and 1.94 Å, respectively (Figures 2D, 3B, and 4D). 3,4-Di-*O*-caffeoylquinic acid interacts with *Ld*NH and *Ld*PTR1 by five and six intermolecular hydrogen bonds having bond lengths of 3.10, 1.99, 2.68, 2.52, and 2.87; and 2.49. 2.46, 1.96, 2.59, 2.15, and 1.77 Å respectively (Figures 3C and 4B).

3.2. *C. fistula* Leaf Extract Inhibited the Growth of *L. donovani*. It was found that *C. fistula* treatment reduced the promastigote proliferation in a time- and dose-dependent manner. The IC_{50} value of *C. fistula* leaf methanolic extract was determined by incubating the parasites at different concentrations including 250, 125, 62.5, 31.25, 15.62, 7.81, and 3.90 μg/mL. By extrapolating the dose−response curve, the IC_{50} value was found to be 43.31 ± 4.202 μg/mL (Figure 5B).

3.3. Cytotoxicity Evaluation of *C. fistula* Leaf Extract. To evaluate the cytotoxic effect of *C. fistula* leaf methanolic extract, THP-1 differentiated macrophages were incubated at twofold serial dilution (0−1000 μg/mL), and the viability was assessed by the MTT assay. *C. fistula* was found safe and least cytotoxic on human macrophages with a CC_{50} of 626 ± 39 μg/mL, while the standard available control drug miltefosine has a CC_{50} value of 7.133 ± 0.65 μg/mL (Figure 5A).

3.4. Effect of *C. fistula* Leaf Extract on the Intra-macrophagic Parasites. After infection, *L. donovani* parasites internalize inside macrophages and transform into amastigotes form. These amastigotes are nonmotile and define the parasite pathogenicity. These amastigote phase parasites are in the clinically relevant form, so it is important to check the effect of *C. fistula* extract on them. THP-1 differentiated macrophages were infected by *L. donovani* promastigotes for 24 h and then treated with different doses of the extract. The extract showed a dose-dependent reduction in parasite burden with an IC_{50} value of 80.76 ± 3.626 μg/mL (Figure 5C). Miltefosine was taken as a positive control. A significant reduction in the amastigote count was observed in the micrographs of infected but extract-treated macrophages (Figure 5D).

3.5. *C. fistula* Leaf Extract Induced Apoptosis in Parasites *In Vitro*. Further, to evaluate whether *C. fistula*-mediated antileishmanial activity was based on apoptosis induction in parasites, we performed the annexin V/PI apoptosis assay. Parasites were treated with different concentrations of methanolic leaf extract for 48 h and then stained and analyzed through a flow cytometer. At 62.5 μg/mL concentration of extract, 8.2% of parasites were found in the early apoptotic phase and 14.3% in the late apoptotic phase (Figure 6). At 125 μg/mL treatment, there were 5.1% cells in the early apoptotic phase and 16.6% cells in the late apoptotic phase (Figure 6). Plant extract induced apoptosis in parasites in a dose-dependent manner. It is also observed that shifting from early to late apoptotic was in a dose-dependent manner. This result suggested that *C. fistula* exerts antileishmanial activity partially through the induction of apoptosis in parasites.

4. DISCUSSIONS

Plants extracts have promising medicinal properties and had been used in the traditional system of medicine. The available ethnopharmacological data of different identified medicinal plants and their secondary metabolites have enormous potential

https://dx.doi.org/10.1021/acsomega.0c05629
ACS Omega 2021, 6, 2318−2327

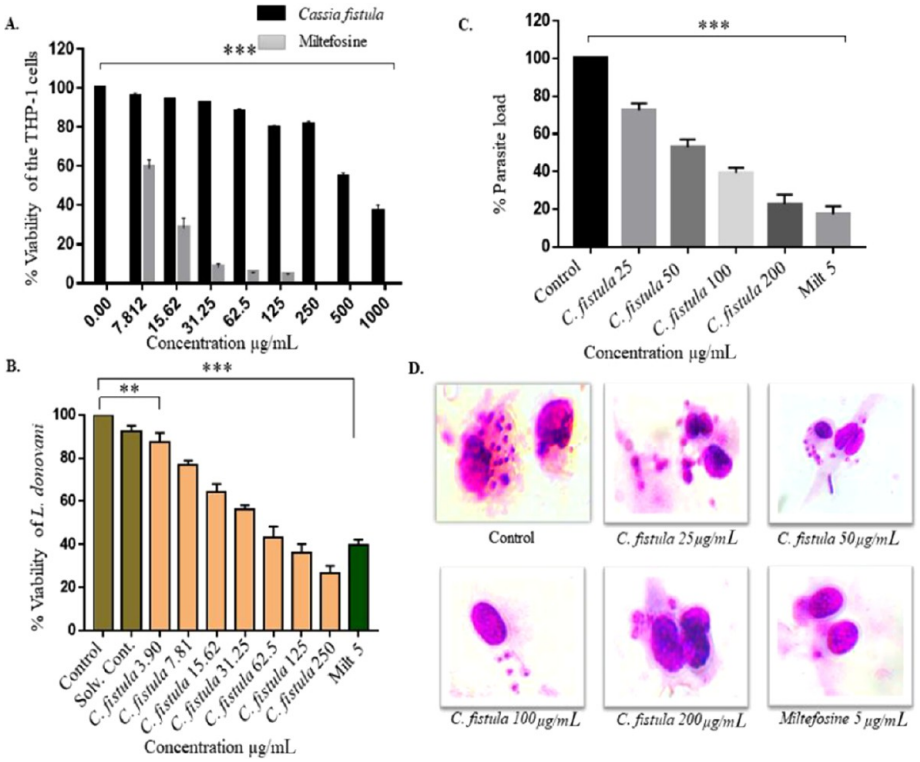

Figure 5. Antileishmanial activity of *C. fistula* leaf extract: (A) THP-1-differentiated macrophages were treated with different concentrations of *C. fistula* and miltefosine (0−1000 μg/mL) and cell viability was ascertained by MTT assay. (B) 5×10^6 stationary phase *L. donovani* promastigotes were treated with different concentrations of *C. fistula* leaf methanolic extracts, with miltefosine-treated positive control and untreated control. Each set is statistically significant compared to control. (C) THP-1-differentiated macrophages were parasitized in a 1:10 ratio with stationary phase promastigotes and then treated with different concentrations of *C. fistula* leaf extract. Percent reduction in the parasite load was determined as described in the method. (D) Intramacrophagic parasites were stained with modified Giemsa stain. The images were captured at 100X under oil immersion.

for the discovery of cost-effective, low cytotoxic, and potential antileishmanial drugs.[39−41] The *C. fistula* plant has plenty of medicinal values. It has been reported to have antibacterial, antifungal, antiviral, and antioxidant activities.[42,43] It has been used to treat tuberculosis, rheumatism, leprosy, syphilis, and skin disease.[44] There has been an exponential growth in the study of primary and secondary metabolite compositions of *C. fistula* in the last few years, which are responsible for most of its attributed biological effects.[13] There are around 12 glycosylated phenolic compounds (including one lignan, two phenolic acids, and nine flavonoids) reported in its leaf extract yet (Table 2). These phytochemicals were selected for *in silico* docking study against unique drug targets of *L. donovani*. Proanthocyanidin B dimer, kaempferol rhamnosylxyloside, myricetin hexoside, apigenin-6,8-di-C-glycoside, apigenin-C-hexoside-O-pentoside, and 3,4-di-O-caffeoylquinic acid showed binding affinity toward the drug targets of *L. donovani*. Proanthocyanidin B dimer and kaempferol rhamnosylxyloside showed the highest binding affinity toward *Ld*SMT, *Ld*TR, *Ld*NH, and *Ld*PTR1. The predicted inhibition constants of proanthocyanidin B dimer against *Ld*SMT, *Ld*TR, *Ld*NH, and *Ld*PTR1 are calculated as 6.92 μM, 6.18 μM, 5.74 μM, and 5.00 μM respectively (Table 1). Molecular docking results suggested possible antileishmanial activity of *C. fistula*. In the light of *in silico* results and medicinal values including antimicrobial activities, we further evaluated its leishmanicidal activities *in vitro*. Methanolic extract of *C. fistula* leaves was found effective on promastigotes as well as intramacrophagic amastigote forms in a dose-dependent manner. Leaf extract was found very much safe against human THP-1-derived macrophages with a very high CC_{50} value of 626 ± 39 μg/mL. Although the positive control, an existing antileishmanial drug, miltefosine was found relatively more toxic on human macrophages as reported by others as well as by us (CC_{50} = 7.133 ± 0.65 μg/mL). The exact mechanism of the antileishmanial activity of *C. fistula* extract was not dissected in detail, but our apoptotic assay suggested partial induction of apoptosis in parasites upon treatment. The number of dead parasites and the percentage of apoptotic cells are not correlated, which suggested the other possible mechanism of antileishmanial activity of the extract.

5. CONCLUSIONS

The *in silico* data suggested that phytoconstituents possibly inhibited the key drug targets of *L. donovani*, which are important for their growth and survival. Further detailed studies are required to work out the exact mechanism of antileishmanial action of the *C. fistula* leaf extract *in vitro* as well as *in vivo*. Our findings may be helpful for designing of the treatment of leishmaniasis through the use of *C. fistula* alone or in combination with the existing antileishmanial drugs.

■ ASSOCIATED CONTENT

Supporting Information

The Supporting Information is available free of charge at https://pubs.acs.org/doi/10.1021/acsomega.0c05629.

Three-dimensional cartoons and topology maps of *Ld*SMT, *Ld*TR, and *Ld*NH, and template structures

https://dx.doi.org/10.1021/acsomega.0c05629
ACS Omega 2021, 6, 2318−2327

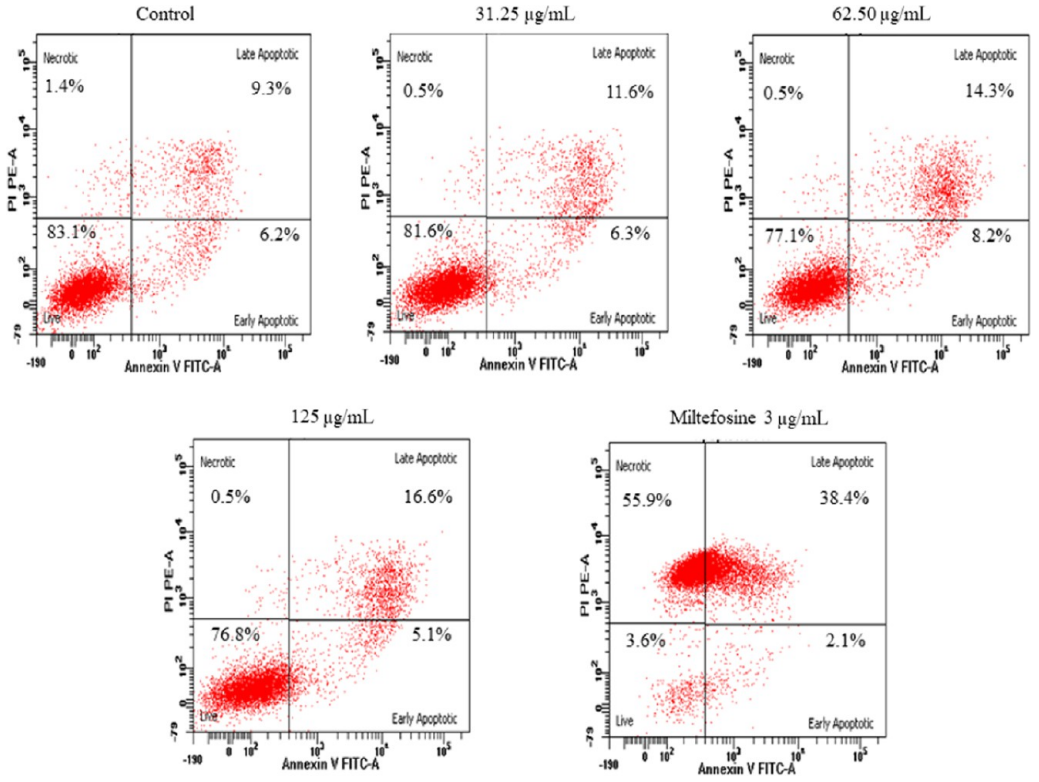

Figure 6. Proapoptotic evaluation of *C. fistula* methanolic extract: *L. donovani* promastigotes were treated with different concentrations of *C. fistula* leaf extract and miltefosine for 48 h and dual-stained with FITC-Annexin V and PI. The bottom left quadrant represents the live parasites, top left PI-stained—necrotic, and bottom right represents the early apoptotic and the top right late apoptotic parasites.

Table 2. Phytochemicals Reported in *C. fistula* Leaf Extract[15]

s. no.	phytochemicals	molecular formula	class of compound
1	syringaresinol	$C_{22}H_{26}O_8$	lignan
2	quercetin-*O*-hexoside	$C_{21}H_{20}O_{12}$	flavonoid
3	apigenin-6,8-di-*C*-glycoside	$C_{27}H_{30}O_{15}$	flavonoid
4	kaempferol rhamnosylxyloside	$C_{26}H_{28}O_{14}$	flavonoid
5	coumaric acid derivative	-	phenolic acid
6	apigenin-6-*C*-pentoside-8-*C*-hexoside (isomer 1)	$C_{26}H_{28}O_{14}$	flavonoid
7	apigenin-6-*C*-pentoside-8-*C*-hexoside (isomer 2)	$C_{26}H_{28}O_{14}$	flavonoid
8	apigenin-6-*C*-pentoside-8-*C*-hexoside (isomer 3)	$C_{26}H_{28}O_{14}$	flavonoid
9	apigenin-*C*-hexoside-*O*-pentoside	$C_{26}H_{28}O_{14}$	flavonoid
10	myricetin hexoside	$C_{21}H_{20}O_{13}$	flavonoid
11	proanthocyanidin B dimer	$C_{30}H_{26}O_{12}$	flavonoid
12	3,4-di-*O*-caffeoylquinic acid	$C_{25}H_{24}O_{12}$	phenolic acid

used for homology modeling of target proteins of *L. donovani* (PDF)

AUTHOR INFORMATION

Corresponding Author

Abdur Rub − *Infection and Immunity Lab (414), Department of Biotechnology, Jamia Millia Islamia (A Central University), New Delhi 110025, India;* orcid.org/0000-0003-1301-0761; Phone: +91-9560887383; Email: arub@jmi.ac.in

Authors

Shams Tabrez − *Infection and Immunity Lab (414), Department of Biotechnology, Jamia Millia Islamia (A Central University), New Delhi 110025, India*

Fazlur Rahman − *Infection and Immunity Lab (414), Department of Biotechnology, Jamia Millia Islamia (A Central University), New Delhi 110025, India*

Rahat Ali − *Infection and Immunity Lab (414), Department of Biotechnology, Jamia Millia Islamia (A Central University), New Delhi 110025, India*

Abdulaziz S. Alouffi − *King Abdulaziz City for Science and Technology, Riyadh 11442, Saudi Arabia*

Bader Mohammed Alshehri − *Department of Medical Laboratory Sciences, College of Applied Medical Sciences, Majmaah University, Al Majmaah 11952, Saudi Arabia*

Fahdah Ayed Alshammari − *College of Sciences and Literature Microbiology, Northern Border University, Arar 73222, Saudi Arabia*

Mohammed A. Alaidarous − *Department of Medical Laboratory Sciences, College of Applied Medical Sciences,*

https://dx.doi.org/10.1021/acsomega.0c05629
ACS Omega 2021, 6, 2318−2327

Majmaah University, Al Majmaah 11952, Saudi Arabia; Health and Basic Sciences Research Center, Majmaah University, Al Majmaah 15341, Saudi Arabia

Saeed Banawas − *Department of Medical Laboratory Sciences, College of Applied Medical Sciences, Majmaah University, Al Majmaah 11952, Saudi Arabia; Health and Basic Sciences Research Center, Majmaah University, Al Majmaah 15341, Saudi Arabia; Department of Biomedical Sciences, Oregon State University, Corvallis, Oregon 97331, United States*

Abdul Aziz Bin Dukhyil − *Department of Medical Laboratory Sciences, College of Applied Medical Sciences, Majmaah University, Al Majmaah 11952, Saudi Arabia; Health and Basic Sciences Research Center, Majmaah University, Al Majmaah 15341, Saudi Arabia*

Complete contact information is available at: https://pubs.acs.org/10.1021/acsomega.0c05629

Funding

The authors thank the Deanship of Scientific Research at Majmaah University, Al Majmaah, 11952, Saudi Arabia, for supporting this work under the Group Project Number RGP-2019-31. The authors are also thankful to the Ministry of Ayush for funding (Z.28015/252/2016-HPC (EMR)-AYUSH-C).

Notes

The authors declare no competing financial interest.

■ ACKNOWLEDGMENTS

The authors are thankful to the Central Instrumentation Facility, Jamia Millia Islamia, for support.

■ REFERENCES

(1) Bates, P. A. Revising Leishmania's life cycle. *Nat. Microbiol.* **2018**, *3*, 529−530.

(2) Walters, L. L.; Irons, K. P.; Chaplin, G.; Tesh, R. B. Life cycle of Leishmania major (Kinetoplastida: Trypanosomatidae) in the neotropical sand fly Lutzomyia longipalpis (Diptera: Psychodidae). *J. Med. Entomol.* **1993**, *30*, 699−718.

(3) Alvar, J.; Vélez, I. D.; Bern, C.; Herrero, M.; Desjeux, P.; Cano, J.; Jannin, J.; den Boer, M. Leishmaniasis worldwide and global estimates of its incidence. *PLoS One* **2012**, *7*, No. e35671.

(4) Searo, W. *Regional Strategic Framework for Elimination of Kala-azar from South-East Asia Region (2005−2015)*; World Health Organization, Regional Office for South-East Asia: New Delhi, India, 2005. http://apps.searo.who.int/pds_docs/B0211.pdf.

(5) Sundar, S.; Singh, A.; Rai, M.; Prajapati, V. K.; Singh, A. K.; Ostyn, B.; Boelaert, M.; Dujardin, J. C.; Chakravarty, J. Efficacy of miltefosine in the treatment of visceral leishmaniasis in India after a decade of use. *Clin. Infect. Dis.* **2012**, *55*, 543−550.

(6) Burza, S.; Sinha, P. K.; Mahajan, R.; Lima, M. A.; Mitra, G.; Verma, N.; Balasegaram, M.; Das, P. Risk factors for visceral leishmaniasis relapse in immunocompetent patients following treatment with 20 mg/kg liposomal amphotericin B (Ambisome) in Bihar, India. *PLoS Neglected Trop. Dis.* **2014**, *8*, No. e2536.

(7) Ouakad, M.; Vanaerschot, M.; Rijal, S.; Sundar, S.; Speybroeck, N.; Kestens, L.; Boel, L.; De Doncker, S.; Maes, I.; Decuypere, S.; Dujardin, J. C. Increased metacyclogenesis of antimony-resistant *Leishmania donovani* clinical lines. *Parasitology* **2011**, *138*, 1392−1399.

(8) Rahmani, A. H. *Cassia fistula* Linn: Potential candidate in the health management. *Pharmacogn. Res.* **2015**, *7*, 217−224.

(9) Yadav, R.; Jain, G. C. Antifertility effect of aqueous extract of seeds of *Cassia fistula* in female rats. *Adv. contracept.* **1999**, *15*, 293−301.

(10) Panda, S. K.; Padhi, L. P.; Mohanty, G. Antibacterial activities and phytochemical analysis of *Cassia fistula* (Linn.) leaf. *J. Adv. Pharm. Technol. Res.* **2011**, *2*, 62−67.

(11) Vasudevan, D. T.; Dinesh, K. R.; Gopalakrishnan, S.; Sreekanth, S.; Sonal, S. The potential of aqueous and isolated fraction from leaves of *Cassia fistula* Linn as antibacterial agent. *Int. J. Chem. Sci.* **2009**, *7*, 2363−2367.

(12) Kumar, K.; Satish, S.; Sayeed, I.; Hedge, K. Therapeutic Uses of *Cassia fistula*: Review. *Int. J. Pharm. Chem. Res.* **2017**, *3*, 38−43.

(13) Thirumal, M.; Srimanthula, S.; Kishore, G. *Cassia fistula* Linn-Pharmacognostical, phytochemical and pharmacological review. *Crit. Rev. Pharm. Sci.* **2012**, *1*, 43−65.

(14) Senthil Kumar, M.; Sripriya, R.; Vijaya Raghavan, H.; Sehgal, P. K. Wound healing potential of *Cassia fistula* on infected albino rat model. *J. Surg. Res.* **2006**, *131*, 283−289.

(15) Castro-Lopez, C.; Rojas, R.; Martínez-Avila, G. Screening of the *Cassia fistula* Phytochemical Constituents by UPLC-ESI-QTOF-MS2. *Clin. Oncol.* **2018**, *3*, 1477.

(16) Pei, K.; Ou, J.; Huang, J.; Ou, S. p-Coumaric acid and its conjugates: dietary sources, pharmacokinetic properties and biological activities. *J. Sci. Food Agric.* **2016**, *96*, 2952−2962.

(17) Monzote, L.; Córdova, W. H. P.; García, M.; Piñón, A.; Setzer, W. N. In-vitro and In-vivo Activities of Phenolic Compounds A gainst Cutaneous Leishmaniasis. *Rec. Nat. Prod.* **2016**, *10*, 269.

(18) Costa, R. S.; Souza Filho, O. P.; Dias Júnior, O.; Silva, J. J.; Hyaric, M. L.; Santos, M. A.; Velozo, E. S. In vitro antileishmanial and antitrypanosomal activity of compounds isolated from the roots of Zanthoxylum tingoassuiba. *Rev. Bras. Farmacogn.* **2018**, *28*, 551−558.

(19) Semwal, D. K.; Semwal, R. B.; Combrinck, S.; Viljoen, A. Myricetin: A Dietary Molecule with Diverse Biological Activities. *Nutrients* **2016**, *8*, 90.

(20) Kubata, B. K.; Nagamune, K.; Murakami, N.; Merkel, P.; Kabututu, Z.; Martin, S. K.; Kalulu, T. M.; Huq, M.; Yoshida, M.; Ohnishi-Kameyama, M.; Kinoshita, T.; Duszenko, M.; Urade, Y. Kola acuminata proanthocyanidins: a class of anti-trypanosomal compounds effective against Trypanosoma brucei. *Int. J. Parasitol.* **2005**, *35*, 91−103.

(21) Cheuka, P. M.; Mayoka, G.; Mutai, P.; Chibale, K. The Role of Natural Products in Drug Discovery and Development against Neglected Tropical Diseases. *Molecules* **2016**, *22*, No. 58.

(22) Kumar, P.; Kumar, A.; Verma, S. S.; Dwivedi, N.; Singh, N.; Siddiqi, M. I.; Tripathi, R. P.; Dube, A.; Singh, N. *Leishmania donovani* pteridine reductase 1: biochemical properties and structure-modeling studies. *Exp. Parasitol.* **2008**, *120*, 73−79.

(23) Baiocco, P.; Colotti, G.; Franceschini, S.; Ilari, A. Molecular basis of antimony treatment in leishmaniasis. *J. Med. Chem.* **2009**, *52*, 2603−2612.

(24) Mukherjee, S.; Xu, W.; Hsu, F. F.; Patel, J.; Huang, J.; Zhang, K. Sterol methyltransferase is required for optimal mitochondrial function and virulence in Leishmania major. *Mol. Microbiol.* **2019**, *111*, 65−81.

(25) Goto, Y.; Bhatia, A.; Raman, V. S.; Vidal, S. E.; Bertholet, S.; Coler, R. N.; Howard, R. F.; Reed, S. G. Leishmania infantum sterol 24-c-methyltransferase formulated with MPL-SE induces cross-protection against L. major infection. *Vaccine* **2009**, *27*, 2884−2890.

(26) Nico, D.; Gomes, D. C.; Palatnik-de-Sousa, I.; Morrot, A.; Palatnik, M.; Palatnik-de-Sousa, C. B. *Leishmania donovani* Nucleoside Hydrolase Terminal Domains in Cross-Protective Immunotherapy Against Leishmania amazonensis Murine Infection. *Front. Immunol.* **2014**, *5*, 273.

(27) Dallakyan, S.; Olson, A. J. Small-molecule library screening by docking with PyRx. *Methods Mol. Biol.* **2015**, *1263*, 243−250.

(28) Trott, O.; Olson, A. J. AutoDock Vina: improving the speed and accuracy of docking with a new scoring function, efficient optimization, and multithreading. *J. Comput. Chem.* **2010**, *31*, 455−461.

(29) Shamsi, A.; Mohammad, T.; Anwar, S.; AlAjmi, M. F.; Hussain, A.; Rehman, M. T.; Islam, A.; Hassan, M. I. Glecaprevir and Maraviroc are high-affinity inhibitors of SARS-CoV-2 main protease: possible implication in COVID-19 therapy. *Biosci. Rep.* **2020**, *40*, No. 450.

(30) Kashif, M.; Hira, S. K.; Upadhyaya, A.; Gupta, U.; Singh, R.; Paladhi, A.; Khan, F. I.; Rub, A.; Manna, P. P. In silico studies and evaluation of antiparasitic role of a novel pyruvate phosphate dikinase

inhibitor in *Leishmania donovani* infected macrophages. *Int. J. Antimicrob. Agents* **2019**, *53*, 508−514.
(31) Šali, A.; Blundell, T. L. Comparative protein modelling by satisfaction of spatial restraints. *J. Mol. Biol.* **1993**, *234*, 779−815.
(32) Laskowski, R. A.; Rullmannn, J. A.; MacArthur, M. W.; Kaptein, R.; Thornton, J. M. AQUA and PROCHECK-NMR: programs for checking the quality of protein structures solved by NMR. *J. Biomol. NMR* **1996**, *8*, 477−486.
(33) Laskowski, R. A. PDBsum new things. *Nucleic Acids Res.* **2009**, *37*, D355−D359.
(34) Kashif, M.; Tabrez, S.; Husein, A.; Arish, M.; Kalaiarasan, P.; Manna, P. P.; Subbarao, N.; Akhter, Y.; Rub, A. Identification of novel inhibitors against UDP-galactopyranose mutase to combat leishmaniasis. *J. Cell. Biochem.* **2018**, *119*, 2653−2665.
(35) O'Boyle, N. M.; Banck, M.; James, C. A.; Morley, C.; Vandermeersch, T.; Hutchison, G. R. Open Babel: An open chemical toolbox. *J. Cheminf.* **2011**, *3*, 33.
(36) Rappé, A. K.; Casewit, C. J.; Colwell, K.; Goddard, W. A., III; Skiff, W. M. UFF, a full periodic table force field for molecular mechanics and molecular dynamics simulations. *J. Am. Chem. Soc.* **1992**, *114*, 10024−10035.
(37) Raj, S.; Sasidharan, S.; Dubey, V. K.; Saudagar, P. Identification of lead molecules against potential drug target protein MAPK4 from *L. donovani*: An in-silico approach using docking, molecular dynamics and binding free energy calculation. *PLoS One* **2019**, *14*, No. e0221331.
(38) Wadood, A.; Ahmed, N.; Shah, L.; Ahmad, A.; Hassan, H.; Shams, S. In-silico drug design: An approach which revolutionarised the drug discovery process. *OA Drug Des. Delivery* **2013**, *1*, 3.
(39) Farnsworth, N. R. The Role of Ethnopharmacology in Drug Development. In *Ciba Foundation Symposium 154-Bioactive Compounds from Plants: Bioactive Compounds from Plants*, Ciba Foundation Symposium 154; John Wiley & Sons: Chichester, U.K., 1990; pp 2−11.
(40) Chouhan, G.; Islamuddin, M.; Sahal, D.; Afrin, F. Exploring the role of medicinal plant-based immunomodulators for effective therapy of leishmaniasis. *Front. Immunol.* **2014**, *5*, 193.
(41) Tahir, A. E.; Ibrahim, A. M.; Satti, G. M.; Theander, T. G.; Kharazmi, A.; Khalid, S. A. The potential antileishmanial activity of some Sudanese medicinal plants. *Phytother. Res.* **1998**, *12*, 576−579.
(42) Kirtikar, K.; Basu, B. D. *Indian Medicinal Plants*; International Book Distributer, 1918; pp 1038−1063.
(43) Khan, I.; Khanum, I. *Medicinal and Aromatic Plants of India*; Ukkaz Publications: Hyderabad, 2005.
(44) Nagpal, M. A.; Nagpal, N.; Rahar, S.; Shah, G.; Swami, G.; Kapoor, R. Phytochemical investigation of methanolic extract of *Cassia fistula* leaves. *Pharmacogn. J.* **2011**, *3*, 61−69.

https://dx.doi.org/10.1021/acsomega.0c05629
ACS Omega 2021, 6, 2318−2327